Optical properties and photoinduced phenomena in glasses and thin films of system As_2Se_3-As_2Te_3-SnTe

V. PARCHANSKI*, B. FRUMAROVÁ[a], M. FRUMAR, M. HRDLIČKA, MIL. VLČEK[a]
Department of General and Inorganic Chemistry and Research Centre, Faculty of Chemical Technology, University of Pardubice, Czech Republic
[a]*Institute of Macromolecular Chemistry of AS CR, v. v. i., Prague, Czech Republic*

Bulk glasses of system $(As_2Se_3)_{80-x}(As_2Te_3)_x(SnTe)_{20}$ (x = 0, 5, 10, 15, 20) were prepared by melt quenching method from high purity elements. Amorphous thin films were prepared by pulsed laser deposition. The optically and thermally induced changes of basic parameters of thin films $(As_2Se_3)_{80-x}(As_2Te_3)_x(SnTe)_{20}$ were studied using optical transmittance measurements and spectral ellipsometry. The values of refractive index and its third order non-linear coefficient of PLD layers with x = 15 and 20 slightly increased after exposure and even more after annealing near T_g. These values decreased after exposure and increased after annealing in PLD layers with x = 0; 5 and 10. Optical band gap slightly decreased after exposure and annealing near T_g.

(Received January 9, 2012; accepted February 20, 2012)

Keywords: Thin film, Chalcogenides, Optical properties, Photo-induced phenomena

1. Introduction

Chalcogenide thin films are promising materials for many interesting applications due to their physico-chemical properties [1]. Chalcogenide glasses and their thin films are transparent up to middle infrared spectral region depending on their composition [2]. Some of them are sensitive to the exposure by electromagnetic radiation and show a variety of photoinduced phenomena. The reversible and irreversible photoeffects are successfully applied in optical data storage. Amorphous chalcogenides can be also used as optical fibers, fiber amplifiers, solid state lasers, non-linear elements and in many other optical and optoelectronical applications [3-6].

Very important are also thin films of chalcogenides. They can be prepared by several methods. Pulsed laser deposition (PLD) was used in this paper. PLD of thin chalcogenide films has several advantages when compared with classical vacuum evaporation: relative simplicity of the process, nearly stoichiometric transfer of target material to the films, short process time, and easy control of the process by laser operating parameters [7].

The studied system has relatively large glass forming region and forms stable glasses. Glass forming region and thermal properties of bulk glasses were studied by Vassilev et.al. [8]. In this paper, bulk glasses of system $(As_2Se_3)_{80-x}(As_2Te_3)_x(SnTe)_{20}$ were prepared by melt quenching method and thin films were prepared by PLD. The optically and thermally induced changes of PLD films were studied in the frames of systematic studies of amorphous and crystalline selenides and tellurides as optical and data storage materials. Some optical properties of as-deposited PLD thin films were studied in our previous paper [9]. In present paper, we focused our attention on optically and thermally induced changes of PLD thin films studied in [9].

2. Experimental

Bulk glasses of system $(As_2Se_3)_{80-x}(As_2Te_3)_x(SnTe)_{20}$ were prepared by melt quenching method from high-purity elements (99,999%) sealed in evacuated silica ampoules, that were melted in rocking cylinder furnace at the temperature near 970 °C. The melt was cooled in the mixture of cold water and ice.

Amorphous thin films were prepared from glass powder pellets by pulsed laser deposition (KrF excimer laser, λ = 248 nm, Compex 102 Lambda Physik) at the residual pressure about 2×10^{-4} Pa. Power of laser was 200 mJ/pulse, repetition rate was 20 Hz, deposition rate about 0.3 nm/s and density of energy on the target 1.2 J/cm^2. The chalcogenide thin films were deposited onto substrates (chemically cleaned microscope slides) held at room temperature. The substrates rotated during the deposition in order to prevent non-uniform thickness of thin films.

The composition of bulk glasses and thin films was confirmed by energy dispersive X-ray microanalysis (IXRF Systems) combined with scanning electron microscope (JEOL JSM-5500LV).

Films were exposed by radiation of high pressure Xe lamp (I = 250 mW.cm^{-2}) for 15 minutes. Thin films were annealed below T_g for approximately one hour. The T_g was estimated by differential scanning calorimetry (DSC).

Optical transmittance spectra of bulk glasses and thin films were measured with Bio-rad spectrophotometer FTS 175C and with spectrophotometer Jasco V-570. The optical parameters of as-deposited, exposed and thermally

annealed thin films were obtained also from ellipsometric measurements (J.A. Woollam VASE Variable Angle Spectroscopic Ellipsometer) in the spectral range 300 – 2300 nm at 60°, 65° and 70° angles of incidence. The fit of obtained ellipsometric parameters Δ and ψ was done using Tauc-Lorentz model [10]. Basic optical parameters (refractive index, absorption coefficient, optical transmittance) and thickness were obtained using WVASE software 3.668. Optical energy band gap of studied thin films was evaluated also by Tauc method [11].

The structure was studied by Raman spectroscopy using spectrophotometer FT-IR Bruker IFS 55 with Raman module FRA 106. Nd:YAG laser with the wavelength 1064 nm was used as an excitation source. Each spectrum was reduced according to Gammon-Shuker formula to remove the thermal influence on the part of spectrum with low Raman shift. Reduced Raman spectra were normalized to the same intensity of maxima and deconvoluted into several individual bands.

X-ray diffraction (XRD) was performed on Bruker D8 diffractometer in range of angles 2θ from 5° to 65°.

3. Results and discussion

Studied bulk glasses were of black color with strong luster. Deposited thin films were dark brown. The surface of bulk glasses and deposited thin films was smooth as revealed by scanning electron microscopy. Chemical composition of prepared glasses determined by EDX analysis was in good accordance with weighed amounts of elements (Table 1). Deposited thin films were compositionally homogeneous with uniform thickness. Their composition was very close to this one of target materials with small understoichiometry of Te (Table 1).

Table 1. Chemical composition of bulk (bulk) glasses and pulsed laser deposited (PLD) thin films determined by EDX analysis compared with theoretical composition (theor).

	x = 0			x = 5			x = 10			x = 15			x = 20		
	theor	bulk	PLD	theor	bulk	PLD	theor	bulk	PLD	theor	bulk	PLD	theor	bulk	PLD
As	36.5	36.2	35.3	36.5	34.7	34.8	36.5	34.6	34.5	36.5	36.9	38.2	36.5	37.1	38.5
Se	54.5	55.0	56.0	51.0	52.9	54.3	48.0	49.5	51.1	44.5	44.5	45.7	41.0	40.0	42.1
Sn	4.5	4.4	4.6	4.5	4.6	4.1	4.5	4.3	4.1	4.5	4.4	3.8	4.5	4.3	3.6
Te	4.5	4.4	4.1	8.0	7.7	6.8	11.0	11.6	10.4	14.5	14.2	12.5	18.0	18.6	15.8

Short wavelength absorption edge of bulk glasses of system $(As_2Se_3)_{80-x}(As_2Te_3)_x(SnTe)_{20}$ was shifted from 970 nm for x = 0 to 1300 nm for x = 20. The value of optical transmittance in transparent region varied between 50% and 65% for samples with thickness approximately 0.5 mm. Optical band gap of bulk glasses was evaluated from spectral dependencies of absorption coefficient (Fig. 1), because the Tauc formula can be applied in the high absorption region ($\alpha > 10^4$ cm^{-1}). E_g^{opt} of bulk glasses decreased with increasing content of As_2Te_3 from 1.29 eV for x = 0 to 1.06 eV for x = 20 (Table 2).

Table 2. Optical band gap of bulk glasses (determined from α vs. E plot as the energy where α = 50 cm^{-1}).

glass composition	E_g^{opt} [eV]
$(As_2Se_3)_{80}(SnTe)_{20}$	1.29
$(As_2Se_3)_{75}(As_2Te_3)_5(SnTe)_{20}$	1.26
$(As_2Se_3)_{70}(As_2Te_3)_{10}(SnTe)_{20}$	1.20
$(As_2Se_3)_{65}(As_2Te_3)_{15}(SnTe)_{20}$	1.12
$(As_2Se_3)_{60}(As_2Te_3)_{20}(SnTe)_{20}$	1.06

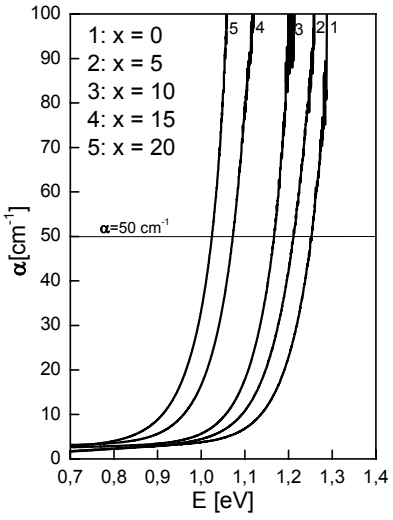

Fig. 1. Spectral dependence of absorption coefficient of bulk glasses of system $(As_2Se_3)_{80-x}(As_2Te_3)_x(SnTe)_{20}$.

Structure of bulk glasses and PLD thin films was studied by Raman spectroscopy in the range of Raman shift between 100 cm^{-1} and 300 cm^{-1} from Rayleigh line. Bulk glasses and PLD thin films showed very similar Raman spectra (Fig. 2,3). The identical position of bands were found and identified in both bulk glasses and PLD films. There is a broad band between 100 cm^{-1} and 290 cm^{-1} in spectra of bulk glasses and PLD films with at least three maxima. For deconvolution we used model of independent oscillators, so we supposed that the vibrations of the structural units are independent on each other. The deconvoluted bands have different width, in order to keep the number of bands as low as possible. The whole deconvolution and the choice of wavenumber should be accepted as the first approximation. The positions of bands were chosen with respect to previously published papers at the wavenumbers where the vibrations of bonds present in studied system were expected. Following Raman bands were used for deconvolution and discussion (Fig. 4). The most intense band in $(As_2Se_3)_{80}(SnSe)_{20}$ glass at 224 cm^{-1} can be assigned to the symmetrical stretching vibration of $AsSe_3$ trigonal pyramids which are connected by their corners [12-14]. The intensity of this band decreased after addition of As_2Te_3 to the system. The shoulder of the main broad band at 272 cm^{-1} can be assigned to the Se-Se vibration in As-Se-Se-As structural units [13,15,16]. The intensities of bands at 242 cm^{-1} and 256 cm^{-1} decreased with increasing content of As_2Te_3. These two bands most probably belong to the vibrations of As_4Se_3 molecules which can be present in the glass [14,17,18]. The bands at 218 cm^{-1} and 206 cm^{-1} appeared after adding of As_2Te_3, we therefore suppose that the glassy system exists as a solid solution of its components and the new structural units $AsSe_xTe_{3-x}$ are created, where one or two atoms of selenium are replaced by tellurium atoms [16,19]. The band at 190 cm^{-1} can be assigned either to the vibrations of $AsTe_3$ pyramids [20] or to the vibrations of As_4Se_3 molecules [17]. Intense sharp band at 185 cm^{-1} is present in glasses with Sn and it corresponds to the A_{1g} vibration observed in crystalline $SnSe_2$. [21,22] The bands found between 120 cm^{-1} and 150 cm^{-1} were also observed in crystalline $SnSe_2$ and SnSe. The bands corresponding to the vibrations of $SnSe_2$ were observed in samples with the content of As_2Te_3 0%, 5% and 10%. The bands arising from the presence of SnSe appeared in glasses and thin films with 15 and 20 % of As_2Te_3. The presence of $SnSe_2$ and SnSe in the glasses annealed near the crystallization temperature was determined by XRD (Fig. 5). We supposed that $SnSe_2$ and SnSe or Sn-Se bonds can be present also in glassy samples. The bands at 163 cm^{-1} and 170 cm^{-1} were observed in the spectra of system Se_xTe_{1-x} [23]. We assume these bands at 163 cm^{-1} and 170 cm^{-1} correspond to the vibrations of Te-Te bonds that connect the pyramidal units of $AsTe_3$, $AsSe_2Te$ or $AsSeTe_2$ [19].

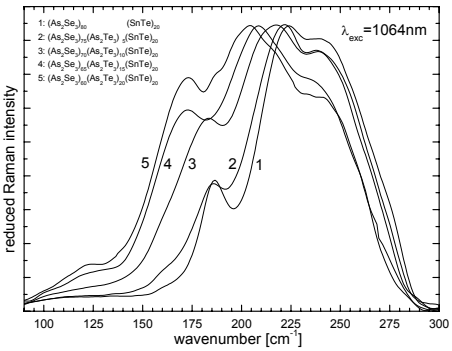

Fig. 2. Reduced Raman spectra of bulk glasses of the system $(As_2Se_3)_{80-x}(As_2Te_3)_x(SnTe)_{20}$.

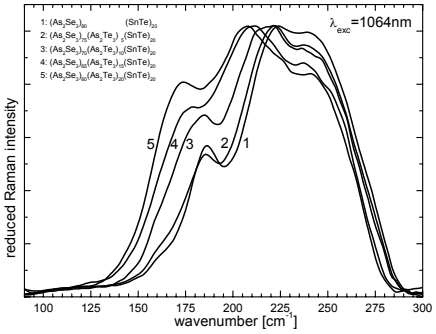

Fig. 3. Reduced Raman spectra of PLD thin films of system $(As_2Se_3)_{80-x}(As_2Te_3)_x(SnTe)_{20}$.

Spectral dependencies of optical transmittance of PLD thin films show interferences typical for thin films. Some optical parameters (refractive index, relative permittivity, linear oscillator energy, dispersion energy, optical band gap and $\chi^{(3)}$ coefficient) of PLD thin films were calculated from positions of interference minima and maxima using Swanepoel method [24] and Wemple-DiDomenico semi-empirical linear oscillator model [25]. Spectral dependencies of refractive index can be described by Cauchy model [26].

The Miller's rule was used for evaluation of third-order non-linear coefficient of refractive index $\chi^{(3)}$ for near-infrared part of spectrum.

$$\chi^{(3)} = \frac{A}{(4\pi)^4}\left(n^2 - 1\right)^4 = \frac{A}{(4\pi)^4}\left(\frac{E_d}{E_0}\right)^4 \qquad (1)$$

where E_0 is linear oscillator energy, E_d is dispersion energy from Wemple-DiDomenico model [25]. The mean value of experimentally found constant A is approximately 1.7 x 10^{-10} (for $\chi^{(3)}$ in esu) [27]. We suppose that this value can be applied also for selenides and tellurides. Third order non-linear coefficient $\chi^{(3)}$ is connected to linear refractive index [27], therefore its spectral dependence shows similar trend. The $\chi^{(3)}$ increased with increasing content of As_2Te_3 as it can be expected [9].

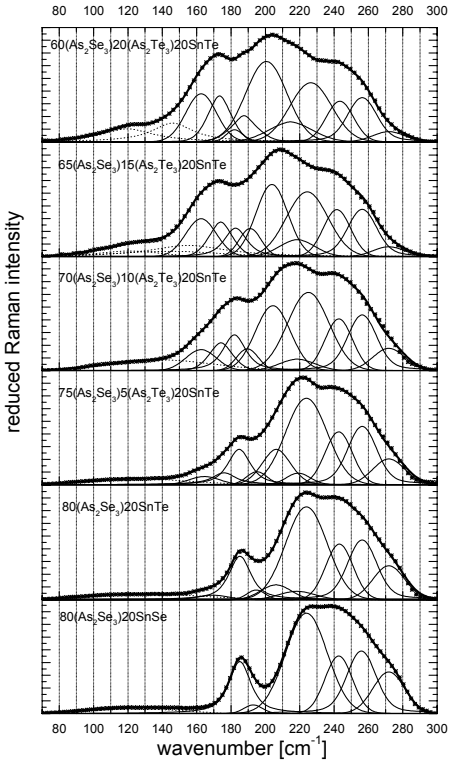

Fig. 4. Deconvoluted reduced Raman spectra of bulk glasses system $(As_2Se_3)_{80-x}(As_2Te_3)_x(SnTe)_{20}$.

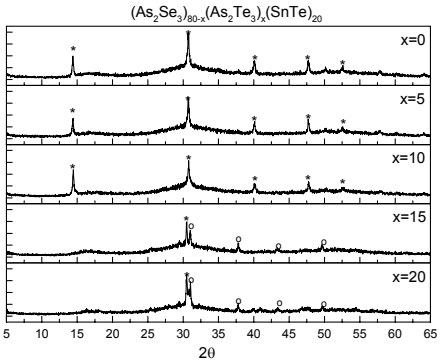

Fig. 5. XRD patterns of samples annealed at the temperature of crystallization. The sharp peaks at 2θ = 15°, 31°, 40°, 48° in samples with x = 0; 5 ;10 were observed in XRD pattern of crystalline $SnSe_2$. The peaks at 2θ = 32°, 38°, 49° in samples with x = 15 and 20 were found in XRD patterns of crystalline SnSe.

The energy band gap of thin films was calculated according to Tauc formula [11]

$$(\alpha h\nu)^n = B^n.(h\nu - E_g^{opt}) \qquad (2)$$

where α is absorption coefficient, hν is energy of light, E_g^{opt} is energy band gap and B is a constant, n is coefficient described in [27].

The short wavelength absorption edge of PLD thin films was shifted to lower energies after annealing near T_g. In films with 15% and 20% of As_2Te_3 it was shifted after exposure (red shift) to lower energies. In other cases shift to higher energies occurred (films with 0%, 5% and 10% As_2Te_3).

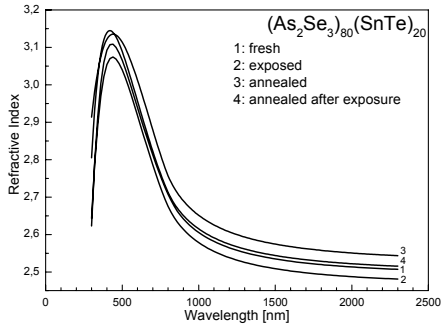

Fig. 6. Spectral dependence of refractive index of PLD thin film and its changes after exposure and thermal annealing.

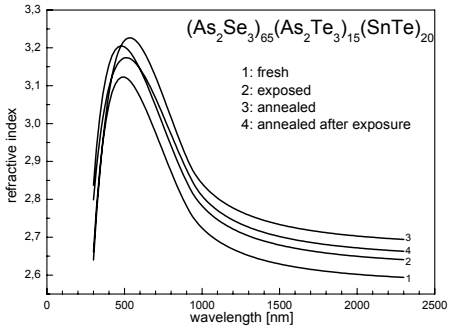

Fig. 7. Spectral dependence of refractive index of PLD thin film and its changes after exposure and thermal annealing.

The refractive index of PLD thin films, determined from ellipsometric data, slightly decreased after exposure of films with 0%, 5% and 10% of As_2Te_3 and increased after annealing (Fig. 6). In the films with higher content of As_2Te_3 (15% and 20%) the refractive index increased after exposure and even more after annealing (Fig. 7). The refractive index has its maximum near 500 nm and then drops to n_0 value in accordance with Cauchy formula

$$n = A + \frac{B}{\lambda^2} + \frac{C}{\lambda^4} \quad (3)$$

where n is refractive index, A (A = n_0), B and C are material dependent constants, λ is the wavelength. The same character of optically and thermally induced changes as in refractive index dependence were observed in spectral dependencies of $\chi^{(3)}$ coefficient (Fig. 8, 9), which is closely connected with linear refractive index [27].

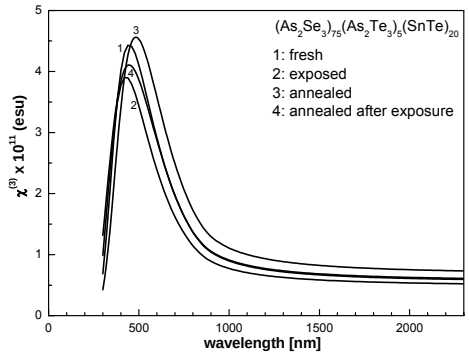

Fig. 8. Spectral dependence of $\chi^{(3)}$ coefficient of PLD thin film and its changes after exposure and thermal annealing.

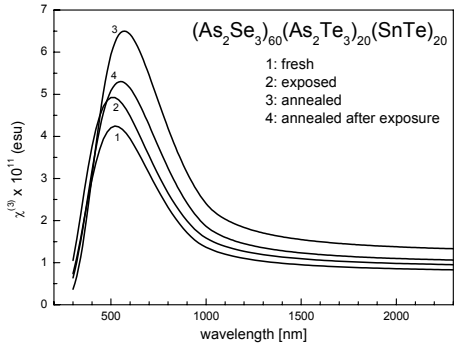

Fig. 9. Spectral dependence of $\chi^{(3)}$ coefficient of PLD thin film and its changes after exposure and thermal annealing.

The changes in $(n^2\text{-}1)^{-1}$ vs. E^2 plots from Wemple-DiDomenico model [25] were observed. The decrease of refractive index after exposure of PLD thin films with 0%, 5% and 10% of As_2Te_3 and its increase after exposure in PLD thin films with 15% and 20% of As_2Te_3 was observed (Table 3). The refractive index increased after annealing in all cases. The linear oscillator energy E_0 of thin amorphous films, calculated from Wemple-DiDomenico model, was not changed by exposure of light, but it was slightly decreased after thermal annealing near T_g as the result of decrease of energy band gap. The changes of dispersion energy of thin films after exposure and after annealing were very small. E_d is the measure of average strength of interband optical transitions and depends on coordination number of cation, formal valency of anion, effective number of valence electrons per anion, etc. Basic optical parameters of PLD thin films (as-deposited, exposed, annealed and annealed after exposure) are listed in Tab 3. These parameters were calculated from ellipsometric data using methods of Swanepoel [24], Wemple-DiDomenico [25] and of Tauc [11].

Energy band gap of PLD thin films increased after exposure by light. It decreased after annealing of as-deposited and exposed thin films. The slope of linear part of Tauc plots was not changed by exposure of light, but it decreased after thermal annealing (Table 3). The same behavior of Tauc's plot slope was observed in As_2S_3 and As_2Se_3 after annealing at the temperature near T_g [28].

Different behavior of exposed PLD thin films with x = 0, 5, 10 (decrease of refractive index, relative permittivity, $\chi^{(3)}$ coefficient) when compared with x = 15, 20 (increase of refractive index, relative permittivity, $\chi^{(3)}$ coefficient) (Table 3) is probably caused by different structure of thin films as determined by Raman spectroscopy. Raman spectroscopy showed that $SnSe_2$ respectively SnSe structural units are present in thin films (see above).

Fresh deposited thin films were not homogeneous and contain material fragments formed during deposition. The material could be less dense with higher free volume; the voids can be present in the structure. After annealing at the temperature near T_g, the structure becomes more stable, voids may disappear, the fragments would disappear due to their chemical interaction. The changes of as-deposited thin films after thermal annealing are irreversible. It can explain changes after thermal annealing of fresh deposited and exposed thin films.

Table 3. Basic physical parameters of PLD thin films. (fr – fresh deposited, ex – exposed, ann – annealed, ex+ann – annealed after exposure)

	$(As_2Se_3)_{80}(SnTe)_{20}$				$(As_2Se_3)_{75}(As_2Te_3)_5(SnTe)_{20}$				$(As_2Se_3)_{70}(As_2Te_3)_{10}(SnTe)_{20}$				$(As_2Se_3)_{65}(As_2Te_3)_{15}(SnTe)_{20}$				$(As_2Se_3)_{60}(As_2Te_3)_{20}(SnTe)_{20}$			
	fr	ex	ann	ex+ann	fr	ex	ann	ex+ann	fr	ex	ann	ex+ann	fr	ex	ann	ex+ann	fr	ex	ann	ex+ann
ε_r	6.18	6.06	6.36	6.22	6.36	6.15	6.60	6.32	6.52	6.29	6.54	6.59	6.59	6.82	7.10	6.94	6.76	6.96	7.45	7.11
n_0	2.49	2.46	2.52	2.49	2.52	2.48	2.57	2.51	2.55	2.51	2.56	2.56	2.57	2.61	2.66	2.63	2.60	2.64	2.73	2.67
E_d [eV]	20.2	19.7	20.1	20.2	20.1	19.5	20.8	19.6	20.0	19.3	19.7	20.2	19.9	20.1	21.1	20.6	19.9	20.4	21.1	20.2
E_0 [eV]	3.9	3.9	3.8	3.9	3.8	3.8	3.7	3.7	3.6	3.6	3.6	3.6	3.6	3.5	3.5	3.5	3.5	3.4	3.3	3.3
$\chi^{(3)}.10^{12}$	4.92	4.45	5.61	5.08	5.62	4.81	6.73	5.44	6.32	5.34	6.44	6.64	6.68	7.85	9.46	8.49	7.51	8.60	11.9	9.52
E_g^{opt}[eV]	1.66	1.73	1.52	1.63	1.60	1.66	1.51	1.57	1.55	1.70	1.50	1.55	1.49	1.54	1.43	1.44	1.41	1.45	1.33	1.32

We suppose that two cases may occur after exposure of PLD thin films:

1. x [As_2Te_3] = 0; 5; 10

Crystals of $SnSe_2$ were found by XRD in glasses annealed at the crystallization temperature, but there were no traces of SnSe crystals in annealed samples (Fig. 5). There are probably photolytic reactions after exposure of thin films which can be schematically described as:

$$2As_2Se_3 + h\nu \rightarrow As_4Se_3 + 3Se \quad (4)$$

$$SnSe_2 + h\nu \rightarrow SnSe + Se \quad (5)$$

2. x [As_2Te_3] = 15; 20

In the glasses with higher content of As_2Te_3 annealed at the temperature of crystallization, the crystals of SnSe were detected by XRD (Fig. 5). The value of the refractive index increased and E_g^{opt} decreased after exposure of thin films with higher content of As_2Te_3 as predicts the Moss' rule. The intensity of Raman bands of As_4Se_3 molecules decreased after exposure and the intensity of Raman bands from Te-Te, $SnSe_2$, Se-Te increased (Fig. 10). We were unable to detect any Raman signal in thermally annealed PLD films; therefore only the changes of Raman spectra of exposed PLD films are discussed. In that case this system is similar to the system $As_{57}Se_{43}$ [17] where the intensity of As_4Se_3 Raman bands also decreased. We suppose that part of As_2Te_3 can be transformed into the $As_2(Se,Te)_3$ during the glass forming process and these $As_2(Se,Te)_3$ units may be dissociated into As_4Se_3. This dissociation is decreased after exposure. However, the changes of the Raman spectra are low and the explanation is only qualitative. These changes are not fully understood yet and further study is required for the detailed explanation.

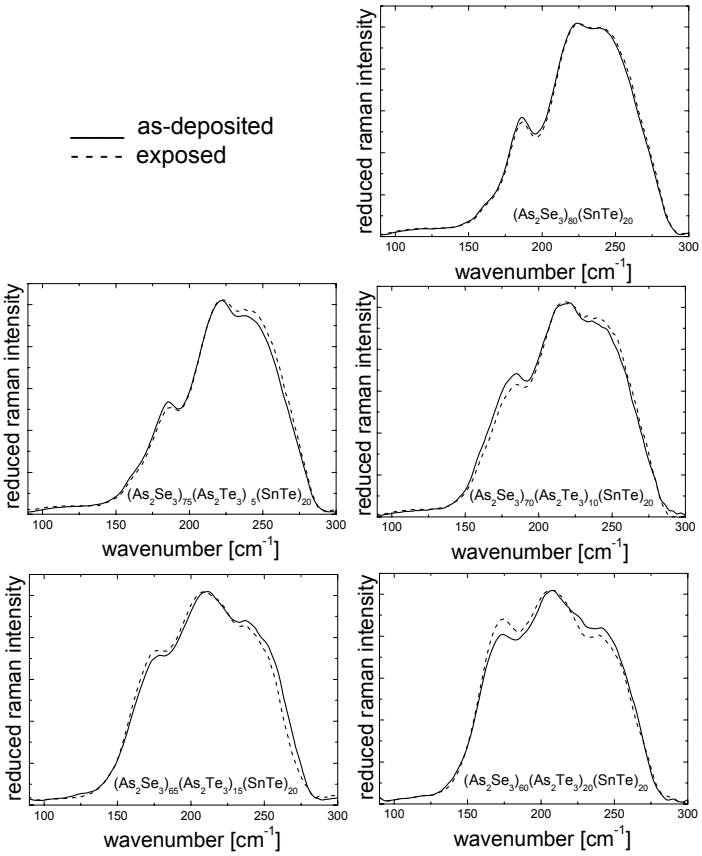

Fig. 10. Reduced Raman spectra of PLD thin films of system $(As_2Se_3)_{80-x}(As_2Te_3)_x(SnTe)_{20}$. full line – as-deposited PLD films; dash line – exposed PLD films.

Different behavior of PLD films after exposure and annealing near T_g may be caused by their different structure. The structural units of $SnSe_2$ were found in samples with 0%, 5% and 10% of As_2Te_3 whereas in the samples with 15% and 20% of As_2Te_3, the units of SnSe were observed (Fig. 5) after annealing at the crystallization temperature.

4. Conclusion

Bulk glasses of system $(As_2Se_3)_{80-x}(As_2Te_3)_x(SnTe)_{20}$ (x = 0, 5, 10, 15 and 20) and their thermally evaporated and pulsed laser deposited thin films were prepared. The structure of bulk glasses and PLD thin films was studied and following structural units were identified from Raman spectra: $AsSe_xTe_{3-x}$ (x = 0; 1; 2; 3), $SnSe_2$, SnSe. The Se-Se and Te-Te bonds that connect the corners of the pyramids were also identified from Raman spectra. EDX microanalysis and Raman spectroscopy proved that PLD method can be very useful for preparing thin films with the same chemical composition and very similar structure as the original bulk glass. Substitution of As_2Se_3 by As_2Te_3 led to decrease of optical band gap in bulk glasses and in thin films and to increase of the refractive index and its third-order non-linear coefficient $\chi^{(3)}$. The increased content of As_2Te_3 lowers the phonon energy and studied glasses can be used as the matrix for near-IR luminescence of rare-earth doped glasses. Studied glasses and thin films can be applied in optics and optoelectronics in infrared spectral region due to large refractive index and $\chi^{(3)}$ coefficient. The refractive index of freshly deposited thin films increased after annealing at the temperature near T_g, which is important for fabrication of optical elements.

Acknowledgement

This research was supported by Grant Agency of Czech Rep. No. GAČR 203/09/0827, project of the Academy of Sci. Czech Rep. AV0Z 40500505 and by Research Centre LC523.

References

[1] J. Zarzycki Materials Science and Technology vol.9. Weinheim VCH (1991).
[2] H. Rawson Properties and Applications of Glass, Amsterdam : Elsevier (1980).
[3] A.V. Kolobov Photo-Induced Metastability in Amorphous Semiconductors. Weinheim : Wiley-VCH (2003).
[4] M. Frumar, M. Vlček, J. Klikorka Reactivity of Solids **4-5,** 341 (1988).
[5] M. Frumar, B. Frumarová, P. Němec, T. Wágner, J. Jedelský, M. Hrdlička J. Non-cryst. Solids. **352,** 544 **(**2006).
[6] J. Oswald, K. Kuldová, B. Frumarová, M. Frumar Mat. Sci. & Eng.:B. **146,** 107 (2008).
[7] M. Frumar, P. Němec, B. Frumarová, T. Wágner Pulsed laser ablation and deposition of chalcogenide thin films. in M. Popescu: Pulsed laser deposition of optoelectronic films. Bucharest : INOE (2005).
[8] V. Vassilev, S. Parvanov, T. Hristova-Vasileva, L. Aljihmani, V. Vachkov, T. Vassileva-Evtimova Matterials Letters. **61**, 3676 **(**2007) .
[9] V. Parchanski, B. Frumarová, M. Frumar, M. Hrdlička, M. Pavlišta, Mil. Vlček J. Non-cryst. solids **355,** 1955 (2009).
[10] G.E. Jellison, F.A. Modine Appl. Phys. Lett. **69**, 371 **(**1996).
[11] J. Tauc Amorphous and Liquid Semiconductors. New York : Plenum (1974).
[12] N. Mateleshko, V. Mitsa, M. Veres, M. Koos Chalcogenide Letters **11,** 139 **(**2004).
[13] T. Mori, S.Onari, T. Arai Japanese J.Appl.Phys. **19,** 1027 (1980).
[14] W. Li J.Appl.Phys. **98** (2005).
[15] F. Charpentier, M. Dussauze, M. Cathelinaud, G. Delaizir J.Alloys and Compounds **509,** 7330 (2011) .
[16] G. Delaizir, M. Dussauze, V. Nazabal, P. Lecante, M. Dollé, P. Rozier, E.I. Kamitsos, P. Jovari, B. Bureau J.Alloys and Compounds **509,** 831 (2011) .
[17] P. Němec, J. Jedelský, M. Frumar, M. Štábl, Z. Černošek Thin Solid Films **484,** 140 (2005) .
[18] M. Ystenes, W. Brockner, F Menzel Vibrational Spectroscopy **5,** 195 **(**1993).
[19] V. Nazabal, M. Cathelinaud, W. Shen, P. Němec, F. Charpentier, H. Lhermite, K.-L. Anne, J. Capoulade, F. Grasset, A. Moreac, S. Inoue, M. Frumar, J.-L. Adam, M. Lequime, C. Amra Applied Optics **47,** 114 **(**2008).
[20] G. Lucovsky, R. M. Martin, J.Non-cryst.Solids. **8-10,** 185 **(**1972).
[21] N.D. Boscher, C.J. Carmalt, R.G Palgrave, I.P Parkin Thin Solid Films. **516,** 4750 **(**2008) .
[22] D.G. Mead, J.C. Irwin Solid State Communications. **20,** 885 **(**1976).
[23] A. Mendoza-Galván, E. García-García, Y.V. Vorobiev, J. González-Hernández Microelectronic Engineerig **51-52** 677 **(**2000) .
[24] R. J. Swanepoel Phys. E **16,** 1214 **(**1983).
[25] S. H. Wemple, M. DiDomenico, Phys. Rev. B **3,** 1338 **(**1971).
[26] A.L. Cauchy Mémoire sur la Dispersion de la Lumière. Praha : Calve (1836).
[27] M. Frumar, J. Jedelský, B. Frumarová, T. Wágner, M. Hrdlička J. Non-cryst. Solids **326&327,** 399 (2003) .
[28] J. Singh Optical Properties of Condensed Matter and Applications, Wiley & Sons (2006).

*Corresponding author: vaclav.parchanski@upce.cz